Influence of the Fe content on the Gd magnetic ordering temperature in $Ni_{1-x}Fe_x$/Gd multilayers

R. Ranchal,[1,*] Y. Choi,[2] M. Romera,[3] J. W. Freeland,[2] J. L. Prieto,[3] and D. Haskel[2]

[1]*Departamento Física de Materiales, Facultad de Ciencias Físicas (UCM), Universidad Complutense de Madrid, Ciudad Universitaria s/n, Madrid 28040, Spain*

[2]*Advanced Photon Source, Argonne National Laboratory, Argonne, Illinois 60439, USA*

[3]*Instituto de Sistemas Optoelectrónicos y Microtecnología and Departamento Física Aplicada, Escuela Técnica Superior de Ingenieros de Telecomunicación, Universidad Politécnica de Madrid, Ciudad Universitaria s/n, Madrid 28040, Spain*

(Received 8 September 2011; revised manuscript received 15 December 2011; published 5 January 2012)

We explore the influence of Fe content on the interfacial magnetic properties of $Ni_{1-x}Fe_x$(50 Å)/Fe (t Å)/Gd(50 Å)/Fe (t Å)/$Ni_{1-x}Fe_x$(50 Å) ($x = 0.2$ and 0.6, and $t = 0$ and 10 Å) multilayers by means of element-specific x-ray magnetic circular dichroism measurements at Gd M_5 and (Ni, Fe) $L_{2,3}$ absorption edges, superconducting quantum interference device magnetometry, and specular reflectivity measurements. Increasing Fe content in the Ni-Fe layer enhances the Gd ordering temperature in the interfacial regions. Addition of a 1-nm Fe spacer results in the largest enhancement in Gd ordering temperature in both interior and interfacial Gd regions, even for high Ni content in the Ni-Fe layer. This indicates that the Fe spacers act as effective barriers (albeit imperfect) in reducing Gd-Ni contact interactions responsible for limiting the interfacial Gd magnetic ordering temperature to values larger than bulk Gd, but significantly lower than observed at Fe/Gd interfaces.

DOI: 10.1103/PhysRevB.85.024403 PACS number(s): 78.70.Dm, 74.78.Fk, 75.70.Cn, 75.50.Bb

I. INTRODUCTION

Magnetic alloys and multilayers consisting of transition metal (TM) and rare-earth (RE) elements exhibit a plethora of interesting magnetic properties stemming from their dissimilar properties. While TMs have strong direct exchange interactions and weakly anisotropic magnetism, REs display weak indirect exchange interactions but strongly anisotropic magnetism (with the exception of isotropic Gd). Furthermore, the sign of exchange coupling between TM $3d$ moments and RE $4f$ moments varies from ferromagnetic (light REs) to antiferromagnetic (heavy REs), providing additional tunability, especially at interfaces.[1] The dissimilar saturation magnetization and Curie temperature of TM and RE layers, together with antiferromagnetic interfacial coupling, causes TM/RE multilayers to exhibit peculiar temperature dependence in magnetization, such as a compensation temperature at which the magnetization reaches a minimum value.[1,2] Among the RE/TM heterostructures, Fe/Gd multilayers have been the most intensively studied systems.[3–10] The absence of diffusion together with a large enhancement of the Gd ordering temperature from 293 K up to ∼1020 K at Gd/Fe interfaces has shown the potential application of these heterostructures.[5]

The combination of Gd and permalloy (or Ni-Fe alloys) has the potential to add additional tunability with implications for future technologies. Recently, permalloy doped with Gd has been used to alter the spin-transfer velocity in magnetic nanostripes,[11,12] which are the base for future racetrack memory technology.[13] The antiferromagnetic coupling between Fe and Gd has also been exploited in permalloy/Gd interfaces[14] and Fe/Gd interfaces[6] to generate in-plane domain walls of great value for fundamental transport studies.

Finally, we should also mention that one of the problems associated with the drastic size reduction of the read heads in hard drives is the enhanced noise coming from the spin transfer torque.[15] Recently, there have been some successful attempts at increasing the critical current for spin transfer torque by including RE impurities in permalloy (Ni-Fe alloys).[16,17] Interestingly, while most lanthanides increase the damping of the permalloy, Gd does not significantly. This situation might be different if the Gd is not introduced as an impurity but rather in a stable trilayer Fe/Gd/Fe heterostructure.

Therefore, while the properties of the Fe/Gd interface have been widely studied, the permalloy/Gd interface is less understood. The potential for tailoring the magnetization, coercivity, and damping properties of the permalloy for future technologies is a main motivator of our study. In particular, it is important to know how efficient a thin Fe layer is for blocking Ni diffusion into the Gd layer.

In this paper, we report on the effect of a changing Ni-Fe composition on the magnetic behavior of Ni-Fe/Gd interfaces. We have measured x-ray magnetic circular dichroism (XMCD) at the $L_{2,3}$ edges of Ni and Fe and the M_5 edge of Gd to probe the $3d$ magnetism of TM and the $4f$ magnetism of Gd, respectively. Our results show that the interfacial Gd magnetism is strongly affected by the composition of the neighboring Ni-Fe layer: increased Fe content in the Ni-Fe alloy promotes the enhancement of the interfacial Gd ordering temperature, with the largest effect observed in samples where a 1-nm Fe spacer is introduced between Gd and Ni-Fe layers.

II. EXPERIMENTAL

The samples were grown at room temperature by sputtering onto oxidized Si(100) substrates. The nominal structure of the multilayers is $Ni_{1-x}Fe_x$(50 Å)/Fe (t Å)/Gd(50 Å)/Fe (t Å)/$Ni_{1-x}Fe_x$(50 Å) ($x = 0.2$ and 0.6, and $t = 0$ and 10 Å). Hereafter, we denote the samples without the Fe spacer layer ($t = 0$ Å) as Ni_8Fe_2 and Ni_4Fe_6 and with the Fe spacer ($t =$ 10 Å) as Ni_8Fe_2/Fe and Ni_4Fe_6/Fe. To protect the samples against oxidation, Ta (30 Å) buffer and Au (50 Å) capping layers have been used. The base pressure was below 6×10^{-8} Torr, and the growth conditions were an Ar pressure of 5 mTorr and a dc power of 20 W for the Gd, 50 W for the Ta, and 60 W for the rest of the layers.

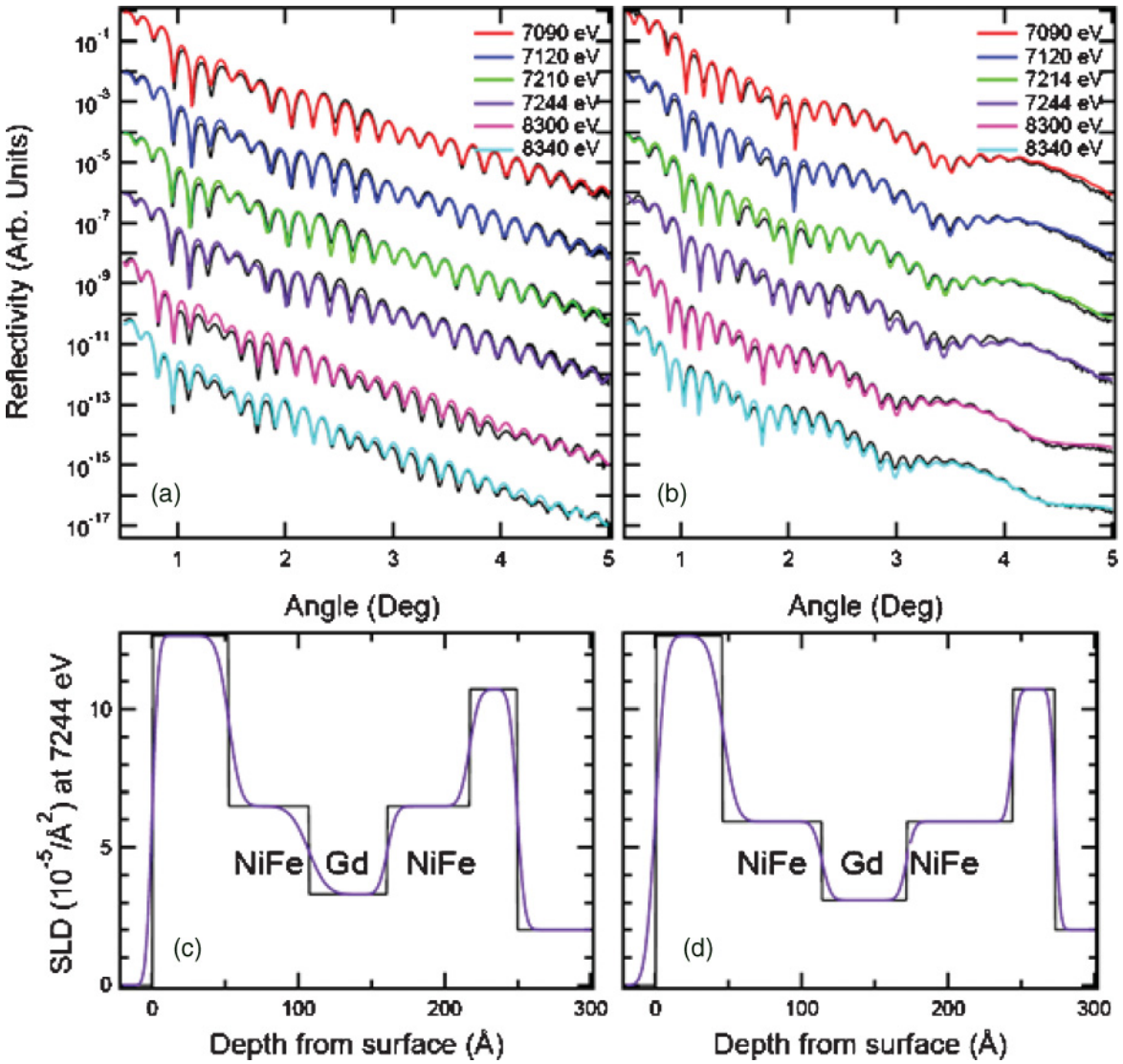

FIG. 1. (Color online) Measured and fitted reflectivity curves at six incident x-ray energies for (a) Ni_8Fe_2 and (b) Ni_4Fe_6. Depth profile of the real part of the scattering length density (SLD) at 7224 eV for (c) Ni_8Fe_2 and (d) Ni_4Fe_6. The lines in black are the fitted SLD profiles before roughness effects are accounted for, and the lines in purple/medium gray are the roughness-convoluted SLD profile.

The magnetic characterization was performed by superconducting quantum interference device (SQUID) magnetometry and XMCD. The film chemical structure was characterized using x-ray reflectivity and x-ray absorption near-edge structure (XANES) spectra measurements at beamline 12-BM of the Advanced Photon Source at Argonne National Laboratory. The XMCD measurements were performed at beamline 4-ID-C of the Advanced Photon Source. X-ray magnetic circular dichroism hysteresis loops were recorded at fixed x-ray helicity at Ni and Fe $L_{2,3}$ edges (851.8 and 707.0 eV, respectively) and at the Gd M_5 edge (1181.8 eV). X-ray magnetic circular dichroism spectra were collected in helicity-switching mode

TABLE I. Thickness (t) and roughness of the bottom side of each layer (ρ) inferred from the x-ray reflectivity fittings. Atomic composition and densities were set to their nominal values in the reflectivity fits. Error bars in fitted values are in the 2–5 Å range.

	Bottom $Ni_{1-x}Fe_x$		Fe interlayer		Gd		Fe interlayer		Top $Ni_{1-x}Fe_x$	
Sample	t (Å)	ρ (Å)	t (Å)	ρ (Å)	t (Å)	ρ (Å)	t (Å)	ρ (Å)	t (Å)	ρ (Å)
Ni_8Fe_2	56.1	5.2			53.9	4.9			54.7	9.1
Ni_8Fe_2/Fe	54.5	6.0	12.1	5.7	57.4	6.2	11.6	4.3	54.2	4.4
Ni_4Fe_6	72.3	3.4			57.8	4.3			67.9	4.8
Ni_4Fe_6/Fe	69.0	3.1	13.8	9.5	55.2	4.7	14.3	10.0	71.7	8.2

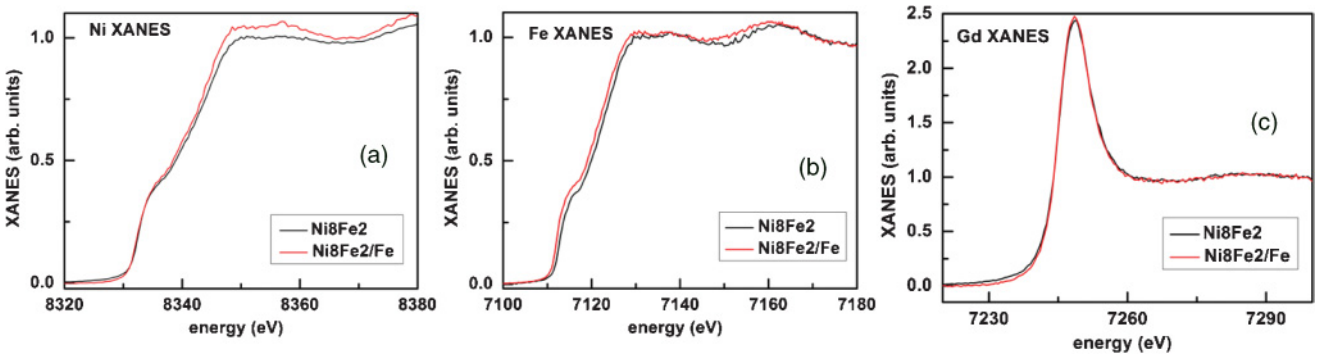

FIG. 2. (Color online) X-ray absorption near-edge structure spectra at the (a) and (b) (Ni, Fe) K edges and (c) Gd L_3 edge. The black line represents the Ni_8Fe_2 sample, while the red/dark gray one is used for the Ni_8Fe_2/Fe sample.

at several temperatures in an external magnetic field of 200 Oe applied parallel to the x-ray wave vector (XMCD measurements were repeated in reversed applied field to verify full sign reversal). The x-ray incident angle was fixed at 10°, and measurements were done in total fluorescence yield (TFY) mode. X-ray magnetic circular dichroism data were collected by recording the helicity-dependent TFY intensities, I^+ and I^-, as a function of incident x-ray energy. Hereafter, we define the XMCD signal as the asymmetry ratio $(I^+ - I^-)/(I^+ + I^-)$. The probing depth of our measurements was such that all magnetic layers contributed to the XMCD signal, as estimated using experimental absorption coefficients previously measured by us for Fe and Ni films and in Ref. 7 for Gd.

III. RESULTS AND DISCUSSION

X-ray reflectivity measurements were performed below and near each of the Gd L_3, Ni K, and Fe K absorption edges, in order to increase elemental sensitivity to Gd, Ni, and Fe in the refined charge density profiles. Grazing incidence reflectivity curves in specular condition were analyzed using Parratt's recursive formula.[18] From the XANES measurements, atomic scattering factors for resonant Gd, Ni, and Fe elements (together with related dispersive corrections δ(E), β(E) to the index of refraction) were obtained. These values were used in the reflectivity analysis along with tabulated scattering factors for nonresonant elements. We used one layer-structure to fit all reflectivity curves measured at the six different on/off edge energy values. Measured and fitted reflectivity curves for Ni_8Fe_2 and Ni_4Fe_6 are shown in Fig. 1, which also shows the scattering length density profiles from the fits with and without roughness. The reflectivity fittings show that individual layers are thicker than nominal values. While the Gd, Ni_8Fe_2, and Fe layers are 2–8 Å thicker, the Ni_4Fe_6 layers are about 20 Å thicker than nominal values (Table I). Since we focus on the magnetism of the Gd/Ni-Fe interface, we expect that variations in Ni-Fe layer thickness from sample to sample would be less critical than variations in the composition of the Ni-Fe layer, the presence (or not) of an Fe interlayer, and the interfacial roughness. We note that the fitted roughness may include contributions from interfacial mixing (random roughness due to interdiffusion) in addition to structural roughness (topological height fluctuation) since their contributions to specular reflectivity cannot be discriminated. Typical Gd, Ni, and Fe XANES spectra are shown in Fig. 2, evidencing the metallic character of all layers with no signatures of oxidation.

We have recorded XMCD hysteresis loops in TFY mode for each element (Ni, Fe, and Gd) at different temperatures

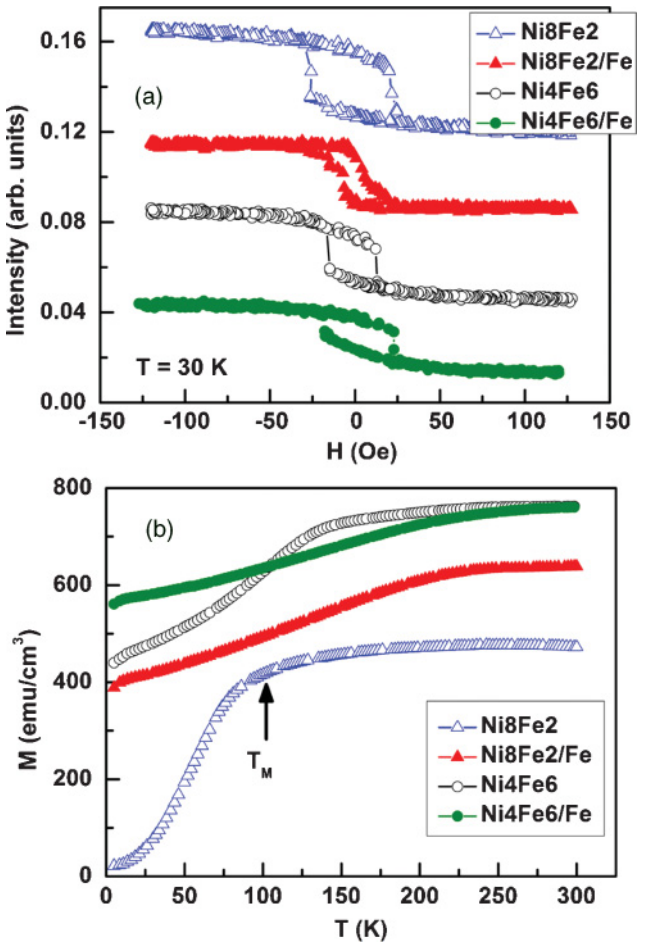

FIG. 3. (Color online) (a) X-ray magnetic circular dichroism hysteresis loops in fluorescence mode measured at the Gd M_5 absorption edge (1181.8 eV) at $T = 30$ K for the samples Ni_8Fe_2 (Δ), Ni_8Fe_2/Fe (▲), Ni_4Fe_6 (○), and Ni_4Fe_6/Fe (●). The loops are shifted vertically for clarity. (b) Temperature-dependent SQUID magnetometry data for the samples Ni_8Fe_2 (Δ), Ni_8Fe_2/Fe (▲), Ni_4Fe_6 (○), and Ni_4Fe_6/Fe (●). We have included as an example the T_M achieved for the sample Ni_8Fe_2.

to analyze the alignment of the magnetic moments relative to the applied magnetic field direction. We present these loops at 30 K because, at this temperature, the Gd magnetization is larger, allowing us to more easily probe for canting of magnetization away from the field direction. The Gd XMCD loops exhibit negligible field dependence between 50 and 150 Oe [Fig. 3(a)]. The Fe and Ni XMCD loops (not shown here) also exhibit flat lines within the same field range. This reveals that Fe, Ni, and Gd magnetic moments remain collinear with the applied field within the field range used in XMCD and SQUID measurements. By collinear, we mean that the (Ni, Fe), and Gd moments are not canted but rather parallel and antiparallel to the field, respectively. At all the studied temperatures, we have observed that the Fe and Ni XMCD loops were inverted in sign relative to Gd XMCD loops, reflecting an antiparallel alignment between the (Fe, Ni) magnetic moments and Gd. Variations in the coercivity seen in Fig. 3(a) are attributed to both extrinsic and intrinsic factors. Namely, the structural quality of the magnetic layers, i.e. the degree of polycrystallinity and roughness of the layers, the magnetic anisotropy of $Ni_{1-x}Fe_x$ and Gd layers, and proximity to the sample's compensation temperature, are all expected to have an effect on the Gd coercivity.

Figure 3(b) shows the temperature dependence of the magnetization measured by a SQUID magnetometer in an applied field of 75 Oe. The magnetization is obtained using the $Ni_{1-x}Fe_x$, Fe, and Gd thicknesses obtained from fits of the x-ray reflectivity. The SQUID measurement is sensitive to the net magnetization from both Ni-Fe (or Ni-Fe/Fe) and Gd layers. The nominal T_C value of bulk Gd is 293 K, while the T_C of Ni-Fe and Fe should be much higher than 300 K. Therefore, the magnetization of Fe and Ni-Fe layers is not expected to show significant temperature dependence below $T = 300$ K. The observed changes in magnetizations in

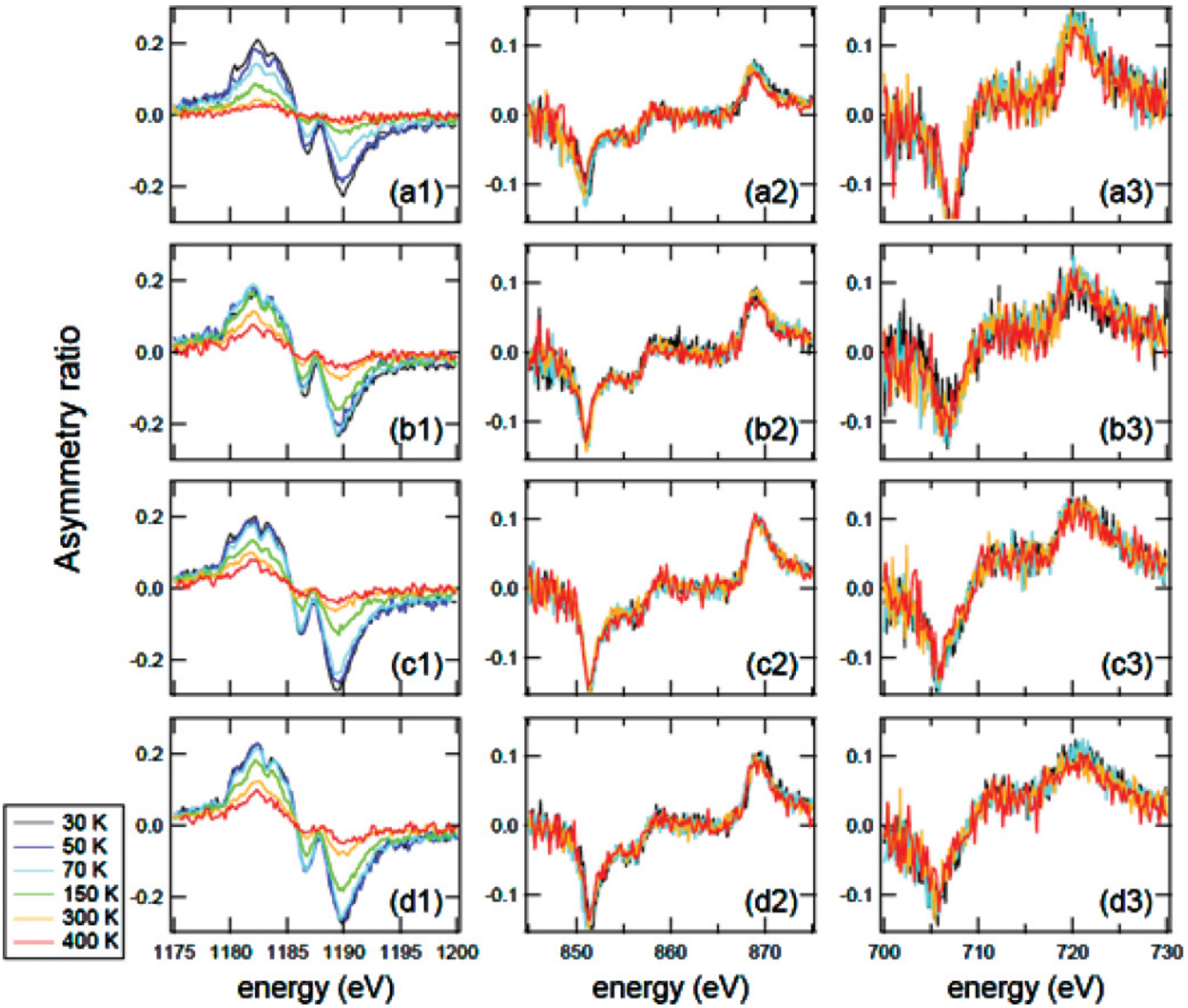

FIG. 4. (Color online) X-ray magnetic circular dichroism spectra across Gd M_5, and (Ni, Fe) $L_{2,3}$ edges at different temperatures. The asymmetry ratios are plotted as a function of the incident x-ray energy for (a) Ni_8Fe_2, (b) Ni_8Fe_2/Fe, (c) Ni_4Fe_6, and (d) Ni_4Fe_6/Fe. The first column reflects the XMCD spectra across the Gd edge M_5 edge, the second column across the Ni $L_{2,3}$ and the third column across the Fe $L_{2,3}$ edge.

Fig. 3(b) can be attributed to changes in Gd magnetization, which decreases significantly as the temperature approaches 300 K. The absence of a compensation temperature down to 5 K, together with a collinear magnetic structure observed in XMCD measurements at 75 Oe shows that the Gd (Ni-Fe) magnetization is aligned antiparallel (parallel) to the applied field at all temperatures in this applied field. We note that a canting of Gd moments, driven by a gain in Zeeman energy, is not likely at temperatures higher than 30 K due to the reduced Gd magnetization. This assignment is confirmed by XMCD measurements showing opposite sign of Gd M_5 and (Ni, Fe) L_3 XMCD signals at all temperatures (Fig. 4).

The SQUID data in Fig. 3(b) show an increase of magnetization up to a certain temperature (T_M) that depends on both the composition of the Ni-Fe layers and the sample layer structure (T_M values summarized in Table II). This T_M has been inferred from the change of slope observed in the temperature dependence of the magnetization. Although TM is qualitatively obtained, it provides a starting point for the two-layer model fittings used in describing the Gd magnetization, as discussed below. The sample with the lowest Fe content (Ni_8Fe_2) also has the lowest T_M, with the net magnetization quickly reaching a plateau as the temperature approaches around 115 K. As the temperature increases further, the net moment continues to increase, albeit at a slower rate. This result suggests the presence of two regions with different temperature response; namely, different ordering temperature. Since we associate the temperature-dependent magnetism of this collinear structure with that of Gd layers, the two temperature regimes with rapidly (slowly) changing magnetization are likely connected with regions within the Gd layer displaying low (high) values of T_C. A similar magnetic configuration has already been reported in Gd/Fe multilayers in which the inner Gd region has a reduced T_C (208 K) from that of bulk Gd (293 K).[5] As the Fe content increases in the layer neighboring the Gd layer by changing the composition of

TABLE II. Magnetization inflection point, T_M, inferred from temperature-dependent SQUID data. Values of ordering temperature for Gd central region (T_{C1}), interfacial region (T_{C2}), and thickness of interfacial regions with enhanced ordering temperature (d_2) inferred from the fitting of Gd-integrated XMCD signal with a two-layer model described in Ref. 5.

Sample	T_M (K)	T_{C1} (K)	T_{C2} (K)	d_2 (Å)
Ni_8Fe_2	115	150	450	10
Ni_8Fe_2/Fe	250	250	450	25
Ni_4Fe_6	140	150	500	18
Ni_4Fe_6/Fe	250	250	550	20

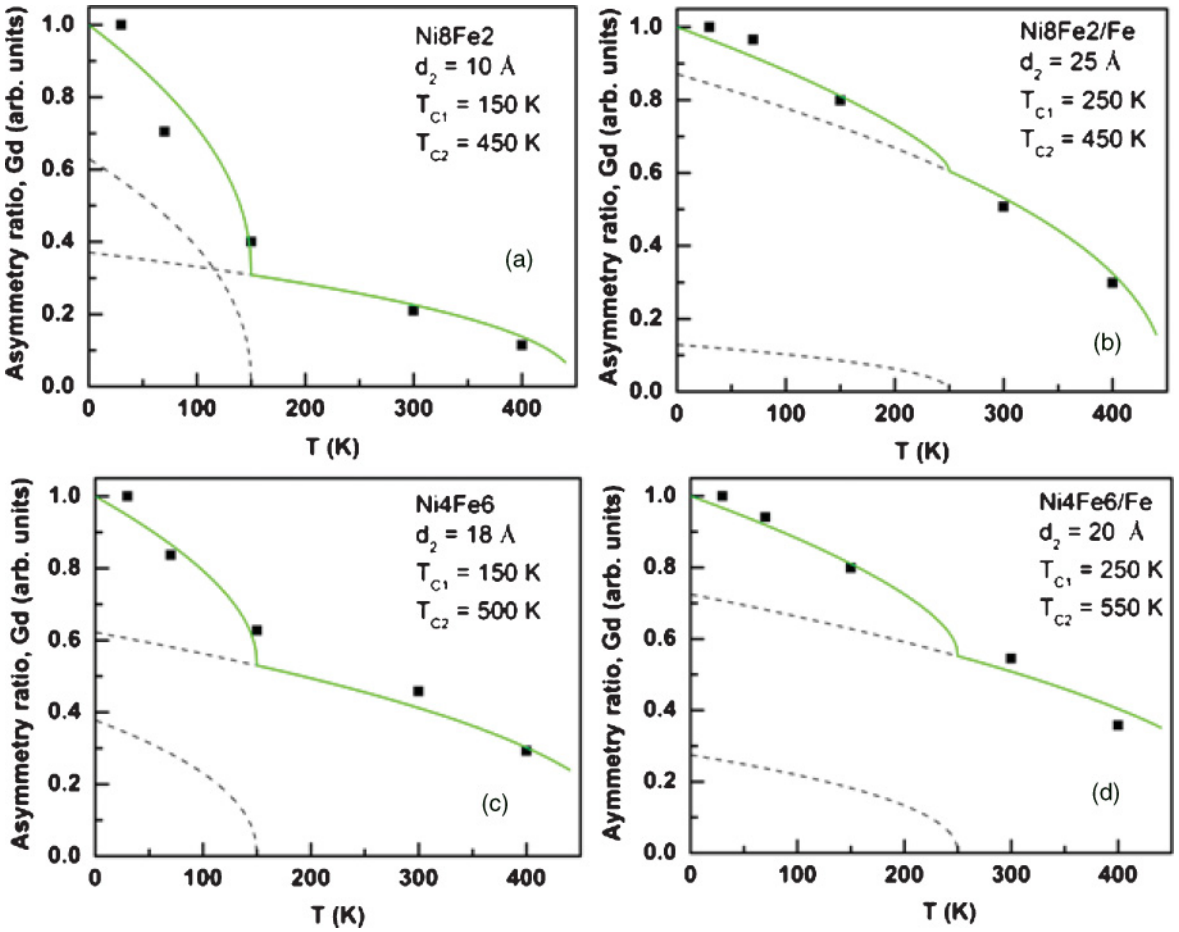

FIG. 5. (Color online) (a)–(d) Gd asymmetry ratio as a function of temperature for all samples. The data have been normalized to T = 30 K in order to fit the data to a two-layer model (Ref. 5). We have included in each graph the parameters inferred from the model, T_{C1}, T_{C2}, and d_2.

the Ni-Fe layer (Ni_4Fe_6) or with the introduction of Fe spacers (Ni_8Fe_2/Fe and Ni_4Fe_6/Fe), the distinction between the two temperature regimes becomes less pronounced. These results indicate that the Gd magnetic ordering is indeed affected by the composition of the neighboring layers. In particular, the temperature dependence of the magnetization in the two samples with Fe spacers is similar despite the different Fe content in the Ni-Fe layers. Therefore, a 1-nm Fe spacer appears to isolate the Gd layer from the Ni-Fe layers.

As already discussed, the temperature dependence of the SQUID data is dominated by the temperature evolution of the Gd layer. In order to clearly investigate this evolution further, we have performed XMCD measurements at the Gd M_5 edge. Figures 5(a)–5(d) show the dependence of the Gd asymmetry ratio on temperature. The Gd XMCD signal persists even up to 400 K, well above the nominal T_C of Gd (293 K). In Fe/Gd multilayers, it has been shown that interfacial Gd regions with enhanced T_C exist near the Fe/Gd interfaces via x-ray resonant magnetic scattering measurements at the Gd L_2 edge.[5,7,10] It has been found that the enhancement of the Gd ordering is localized to the interfacial region so that the T_C of the interfacial region (T_{C2}) is much higher than that of the interior Gd region (T_{C1}).[5] Our observation by XMCD of sizable Gd magnetization above 300 K is consistent with this scenario. As with the SQUID data, XMCD also shows similar temperature dependence for the two samples with the Fe-spacer layer [Figs. 5(b) and 5(d)] and similar behavior for the two samples without the Fe spacer. For the latter, the sample with a Ni_8Fe_2 layer composition has a smaller XMCD signal at 400 K. From these four samples, one can see a clear trend whereby the enhancement of Gd magnetization is strongly correlated with the Fe composition in the neighboring layers ($x = 0.2$, 0.6, and 1).

As seen in Fig. 4, the Ni and Fe XMCD spectra do not change with temperature. Among Gd-Ni alloys, one can find several ferromagnetic phases with Curie temperatures near or below 100 K.[19–21] In these alloys, the observed Ni moment is typically reduced relative to the moment of pure Ni metal. This is not the case, however, in Gd/Ni multilayer films without interfacial alloy formation, where the magnetic moment of Gd was measured by XMCD up to room temperature.[22] Then, the presence of a Gd-Ni alloy, which might be localized at the Ni-Fe/Gd interfaces,[23,24] is not consistent with the observation of Gd magnetization above room temperature in our samples, at least not in a laterally homogeneous sample. In addition, our data show negligible temperature dependence of Ni and Fe XMCD signals, so the presence of Gd-Ni alloys with a low T_C can be ruled out. Any alloy formation as a result of intermixing is likely to be more pronounced in the Ni_8Fe_2 sample, as indicated by the fitted scattering length density (SLD).

We fitted the Gd-integrated XMCD data to a two-layer model[5] in order to separate the ordering temperature of central and interfacial regions. In Fig. 5, the square dots represent the experimental values, whereas the (green/gray) solid lines represent the fits to the two-layer model with the contributions of central and interfacial regions denoted with black, dashed lines. We note that our XMCD data, measured at a single incident angle in TFY mode, cannot provide depth-resolved information on the Gd magnetization. Rather, it provides the Gd magnetization averaged over the probed volume (i.e. the whole Gd layer based on x-ray penetration depth calculations mentioned before). Thus, based on the XMCD data alone, we cannot conclude whether the interfacial Gd region is fully magnetized with the central Gd (interior) region being paramagnetic or if the Gd layer is magnetized uniformly with a reduced magnetization. However, it is reasonable to assume that the Gd region near the Ni-Fe/Gd interfaces is likely to show a different temperature dependence than that of the interior Gd region, where the direct influence from the TM layer is expected to be reduced. We have inferred T_{C1},T_{C2}, and d_2, the latter being the spatial extent of the interfacial region with enhanced ordering temperature. These are also reported in Table II. The Fe content in the neighboring layers affects the ordering temperature of both interior and interfacial regions of the Gd layer. A T_{C1} value of 150 K is found in the samples without Fe spacers, which is enhanced to 250 K in the samples with Fe spacers, close to the Gd bulk value of 293 K. The ordering temperature of interfacial region, T_{C2}, is 450 K in the sample with less Fe content and increases to 550 K as the Fe composition in the neighboring layers ($x = 0.2$, 0.6, and 1) increases. Hence, the introduction of Ni in the $Ni_{1-x}Fe_x$ layers reduces the Gd ordering temperature in the interfacial

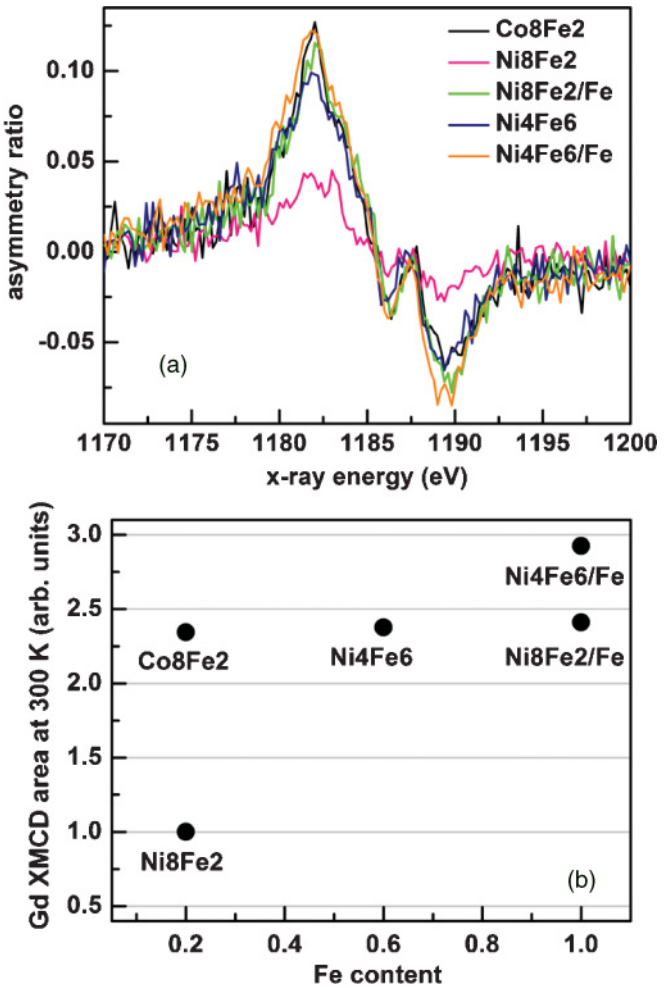

FIG. 6. (Color online) Gd XMCD data at 300 K. (a) Gd XMCD spectra. (b) Areas under the Gd XMCD spectra for samples with different Fe content.

region in comparison to Fe/Gd multilayers where T_{C2} as high as 1020 K was found. From the values of T_{C2}, we can infer a lower interfacial exchange coupling constant relative to that in Fe/Gd multilayers.

In summary, we have studied in detail the evolution of interfacial magnetism in $Ni_{1-x}Fe_x$/Gd heterostructures with varying Ni-Fe composition; in particular, we focus on the effect that an additional Fe spacer has on regulating the magnetization of interior and interfacial regions of Gd layers. For comparison, we have also studied a similar sample where Co_8Fe_2 layers replace the Ni_8Fe_2 layers (Fig. 6). A sizable Gd XMCD signal is evident in this sample at 300 K. The Gd XMCD signal is much larger for Co_8Fe_2 than for Ni_8Fe_2 (same Fe content), indicating that the interfacial exchange coupling is stronger for Gd-Co than for Gd-Ni. This experimental result agrees with results from first-principles calculations[25] where the exchange coupling, J, was found to satisfy $J_{\text{Gd-Fe}} > J_{\text{Gd-Co}} > J_{\text{Gd-Ni}}$. In addition, we have shown that the use of thin Fe spacers is beneficial for heterostructures combining Gd and Ni-Fe layers as a possible means to enhance the exchange coupling between the layers and enhance the Gd magnetization in both interfacial and central regions.

IV. CONCLUSIONS

We have studied the effect of the Fe content on the ordering temperature of Gd layers in $Ni_{1-x}Fe_x$/Gd heterostructures. X-ray magnetic circular dichroism and SQUID magnetometry have shown the presence of two different ordering temperatures in the Gd layer. Regardless of the Fe content, the Gd region closer to the interface exhibits an enhanced Curie temperature above 400 K. This is larger than bulk Gd (293 K) but significantly lower than that found at Fe/Gd interfaces (1020 K). The increase of Fe content in the layers neighboring Gd has a remarkable impact on the magnetic properties of Gd layers. Namely, it not only promotes enhancement of magnetization in interfacial regions, but it also enhances the ordering temperature of the interior of Gd layers. While high Ni content in the Ni-Fe alloy suppresses Gd ordering temperature, it suffices to add a 1-nm Fe spacer to recover (and surpass) the gains in magnetization and ordering temperature achieved by increasing Fe composition in the Ni-Fe alloy. Thus, the Fe-spacer layers act as effective barriers in reducing Gd-Ni interactions that are detrimental to robust Gd magnetization.

ACKNOWLEDGMENTS

This work has been financially supported by the Spanish Ministry of Science through Project MAT2008-02770/NAN and Madrid Regional Government and Universidad Complutense de Madrid through Project CCG10-UCM/MAT-4621. Work at Argonne National Laboratory was supported by US Department of Energy, Office of Science, under Contract No. DE-AC02-06CH11357. M. Romera was funded through the Spanish FPU fellowship AP2007-00464. We thank Nadia Leyarovska for her assistance at beamline 12BM of the Advanced Photon Source, Argonne National Laboratory.

*rociran@fis.ucm.es

[1] R. E. Camley and R. L. Stamps, J. Phys. Condens. Matter **5**, 3727 (1993).
[2] J. P. Andrés, L. Chico, J. Colino, and J. M. Riveiro, Phys. Rev. B **66**, 094424 (2002).
[3] K. Cherifi, C. Dufour, Ph. Bauer, G. Marchal, and Ph. Mangin, Phys. Rev. B **44**, 7733 (1991).
[4] N. Ishimatsu, H. Hashizume, S. Hamada, N. Hosoito, C. S. Nelson, C. T. Venkataraman, G. Srajer, and J. C. Lang, Phys. Rev. B **60**, 9596 (1999).
[5] D. Haskel, G. Srajer, J. C. Lang, J. Pollmann, C. S. Nelson, J. S. Jiang, and S. D. Bader, Phys. Rev. Lett. **87**, 207201 (2001).
[6] J. L. Prieto, B. B. van Aken, G. Burnell, C. Bell, J. E. Evetts, N. Mathur, and M. G. Blamire, Phys. Rev. B **69**, 054436 (2004).
[7] J. F. Peters, J. Miguel, M. A. de Vries, O. M. Toulemonde, J. B. Goedkoop, S. S. Dhesi, and N. B. Brookes, Phys. Rev. B **70**, 224417 (2004).
[8] Y. Choi, D. Haskel, R. E. Camley, D. R. Lee, J. C. Lang, G. Srajer, J. S. Jiang, and S. D. Bader, Phys. Rev. B **70**, 134420 (2004).
[9] Y. Choi, D. Haskel, A. Cady, J. C. Lang, D. R. Lee, G. Srajer, J. S. Jiang, and S. D. Bader, Phys. Rev. B **73**, 174401 (2006).
[10] B. Sanyal, C. Antoniak, T. Burkert, B. Krumme, A. Warland, F. Stromberg, C. Praetorius, K. Fauth, H. Wende, and O. Eriksson, Phys. Rev. Lett. **104**, 156402 (2010).
[11] R. L. Thomas, M. Zhu, C. L. Dennis, V. Misra, and R. D. McMichael, J. Appl. Phys. **110**, 033902 (2011).
[12] S. Lepadatu, J. Claydon, D. Ciudad, A. Naylor, C. Kinane, S. Langridge, S. Dhesi, and C. Marrows, Appl. Phys. Express **3**, 083002 (2010).
[13] S. P. Parkin, M. Hayashi, and L. Thomas, Science **320**, 190 (2008).
[14] J. L. Prieto, M. G. Blamire, and J. E. Evetts, Phys. Rev. Lett. **90**, 027201 (2003).
[15] J. G. Zhu and X. Zhu, IEEE Trans. Magn. **40**, 182 (2004).
[16] G. Woltersdorf, M. Kiessling, G. Meyer, J. U. Thiele, and C. H. Back, Phys. Rev. Lett. **102**, 257602 (2009).
[17] S. G. Reidy, L. Cheng, and W. E. Bailey, Appl. Phys. Lett. **82**, 1254 (2003).
[18] L. G. Parratt, Phys. Rev. **95**, 359 (1954).
[19] T. R. McGuire and R. J. Gambino, IEEE Trans. Magn. Mag. **14**, 838 (1978).
[20] J. Durand and S. J. Poon, IEEE Trans. Magn. Mag. **13**, 1556 (1977).
[21] K. Sato, Y. Isikawa, K. Mori, and T. Miyazaki, J. Appl. Phys. **67**, 5300 (1990).
[22] A. Barth, F. Treubel, M. Marszalek, W. Evenson, O. Hellwig, C. Borschel, M. Albrecht, and G. Schatz, J. Phys. Condens. Matter **20**, 395232 (2008).
[23] R. Ranchal, C. Aroca, and E. López, J. Appl. Phys. **100**, 103903 (2006).
[24] R. Ranchal, C. Aroca, M. C. Sánchez, P. Sánchez, and E. López, Appl. Phys. A **82**, 697 (2006).
[25] X. B. Liu and Z. Altounian, J. Appl. Phys. **107**, 09E117 (2010).